Science Advances
AAAS

Supplementary Materials for

CLEC-1 is a death sensor that limits antigen cross-presentation by dendritic cells and represents a target for cancer immunotherapy

Marion Drouin *et al.*

Corresponding author: Elise Chiffoleau, elise.chiffoleau@univ-nantes.fr

Sci. Adv. **8**, eabo7621 (2022)
DOI: 10.1126/sciadv.abo7621

The PDF file includes:

Other Supplementary Material for this manuscript includes the following:

Supplementary Text

Generation of Fc CLEC-1 proteins

Human and mouse CLEC-1 IgG Fc chimera proteins (Fc CLEC-1) were generated by cloning into pcDNA3.1, the extracellular domain of mouse (Q73-Q269) or human CLEC-1 (Q74-D280) fused in N-terminal to mouse IgG1e2 Fc (Invivogen) or human IgG1e3 Fc (Invivogen) sequences respectively. Synthesis of Fc CLEC-1 sequences was ordered at Genscript with restriction sites XhoI in 5' and XbaI in 3' for cloning in pcDNA3.1. Kozak sequence (GCCACC – SEQ ID No.10) and IgK leader signal peptide (METDTLLLWVLLLWVPGSTGD–SEQ ID No.9) were added in the beginning of the sequences for expression in mammalian cells. Midiprep of plasmid pcDNA3.1 containing Fc CLEC-1 was produced with Nucleobond Xtra Midi EF kit (Macherey Nagel). Recombinant Fc CLEC-1 proteins were produced in 60.10^6 FreeStyle 293-F (HEK) (Thermofisher) by transient transfection with 60µg of plasmid pcDNA3.1-Fc CLEC-1 using 120µl of 293 Fectine transfection reagent (Thermofisher) in 60ml of FreeStyle 293 medium (Thermofisher). After 5 days, supernatant was clarified by centrifugation 30min at 3000g and filtered on 0.22µm Stericup (Merck Millipore) and proteins were purified on HiTrap protein A column (GE) and eluted with 0.1M citric acid pH3. Eluate was concentrated on Microsep Advance10kDa (Pall) and filtered on 0.22µm filter.

Generation of anti-human CLEC-1 mAbs

Hybridomas against human CLEC-1 were generated by Diaclone SAS (Besançon, France) by immunization of mice with human His CLEC-1 (Biotechne) and were selected by ELISA according to conventional protocols. Briefly, 1µg of protein was administered in the foot pad of naive mice, one day per week for three weeks and then one day per two weeks for the last two injections. Draining lymph nodes were collected and hybridomas were obtained by fusing ganglion cells with the mouse myeloma X63/AG.8653 cell line. Hybridomas were selected by their abilities to recognize by flow cytometry cell lines expressing or not CLEC-1. Variable sequence of heavy chain (VH) and light chain (VL) were sequenced and cloned respectively in pcDNA3.4 human IgG4m expression plasmid containing CH1-hinge-CH2-CH3 domains of hIgG4, mutated at S228P to stabilize hinge region and in pcDNA3.4 CLIg-hkappa expression plasmid containing human CLkappa (plasmids from OseImmunotherapeutics, France).

Plasmids were co-transfected in CHO cells and Abs from supernatant (at d7) were purified by Protein A chromatography and quantified by UV (280nm).

Enrichment of CLEC-1 ligand(s) and mass spectrometry

UV-treated Raji and HPB-ALL were lysed in 5 volumes of ice cold mild RIPA-IP lysis buffer (PBS (Corning) containing 1% NP-40, 0.25% Na deoxycholate, 1X Protease Inhibitor cocktail (PIC) (Sigma Aldrich)) followed by 2 cycles of thermal lysis and centrifugation at 14000g (15 min, 4°C) and concentration of whole cell protein extracts (WCE) was determined by BCA assay. For co-IP, protein G Surebeads magnetic beads (Biorad) (resuspended in PBS+0.1% Tween-20 (Sigma-Aldrich)) were coated with Fc-fusion proteins (hFc alone, hFc CLEC-1, or hFc CLEC7A (Invivogen) (1h, 4°C on a rotating wheel) and were added after washing (3 times in PBS-tween and then in PBS) to WCE in cold PBS+1X PIC (3h, 4°C on a rotating wheel). After washing in PBS+500mM NaCl and PBS, eluated proteins (elution buffer (1X Laemmli buffer (Biorad), 250mM DTT (Sigma-Aldrich)), were separated by sodium dodecylsulfate polyacrylamide gel electrophoresis on stain free gels and imaged on a Chemidoc Imaging System (Biorad). Band of interest was cut out in a gel stacking for nanoscale liquid chromatography coupled to tandem mass spectrometry analysis (LSMBO,Strasbourg) performed on a nanoACQUITY Ultra-Performance-LC-system (Waters, Milford, MA) coupled to a TripleTOF 5600 mass spectrometer (ABSciex). Data were analyzed by MASCOT 2.6.2 algorithm (Matrix Science) successively filtered by applying a false discovery rate (FDR) of 1%, and removing the classical contaminants and proteins purified in Fc control and beads only conditions. Eluate was revealed by WB with anti-human TRIM21 mAbs (AB01/1G5, Biorad). Final shortlist was filtered for candidates displaying over 20% sequence coverage and at least 7 specific peptides.

Animals

OT-II.*Ly5.1* homozygous mice were obtained by intercrossing OVA-specific TCR-transgenic OT-II mice (C57BL/6-Tg(TcraTcrb)425Cbn/Crl) (Charles River) with *Ly5.1* mice (B6.SJL-*PtprcaPepcb*/BoyCrl) (Charles River).

RIPmOVA (C57BL/6-Tg (Ins2-TFRC/OVA)296Wehi/WehiJ) transgenic mice *(50)* (6–8 weeks of age) were purchased from The Jackson Laboratory (Bar Harbor, ME), bred heterozygously and screened by PCR for OVA expression according to standard procedure.

Cell lines

Human non-small-cell lung carcinoma (NSCLC) (A549), colorectal cancer (CRC) (DLD-1, HT-29), Ovarian (HeLa), embryonic kidney (HEK293T), hepatocarcinoma (HCC) (HepG2, Huh7), osteosarcoma (U2OS), glioblastoma (U373), T-ALL (Hpb-all, DND41, Jurkat), lymphoma (T2), B-ALL (Raji, Ramos, RPMI8866), myeloma (U266, RPMI8226) and C57Bl/6 mouse mesothelioma (AK-7), hepatocarcinoma (Hepa1.6) and colon adenocarcinoma (MC38) cells were purchased from ATCC or Leibniz Institute DSMZ and cultured according to the manufacturers' instructions in DMEM or RPMI medium (Life Technologies) supplemented with (10% endotoxin-free fetal calf serum (Thermo Fisher), 2 mM L-glutamine (Sigma-Aldrich), 100U/ml Penicillicine; 100µg/ml Streptamycine (Life Tecnologies)) at 37°C and 5% CO_2.

Generation of RIPmOVA bone marrow chimeric mice and induction of autoimmune diabetes

For generation of RIPmOVA chimeric mice, 5.10^6 of bone-marrow cells collected from femurs and tibiae of WT and *Clec1a*-deficient mice and subjected to red blood cell (RBC) lysis (ACK buffer (0.15 M NH_4Cl, 1 mM $KHCO_3$, and 0.1 mM Na_2EDTA (pH 7.4))) were injected i.v. into lethally whole-body X-irradiated (Faxitron CP 160 (Faxitron X-Ray Corp., Wheeling) (day−1, 11 Gy) RIPmOVA recipient mice. Reconstituted mice were injected sc. with Terramycin (200mg/kg) (Sigma-Aldrich) and drinking water was supplemented with neomycin trisulfate (2mg/ml) (Coophavet) for 2 weeks. Eight weeks after reconstitution, chimeras were i.v. injected with 5.10^6 of purified $CD8^+$ T cells ($CD8a^+$ T cell Isolation Kit II, Miltenyi Biotec) from spleens and lymph nodes of OT-I TCR-transgenic mice ± 0.5 mg of anti-OVA polyclonal antibody (IgG from serum of OVA-hyperimmunized rabbits purified by protein A affinity chromatography; Covalab, Villeurbanne, France). Blood glucose levels were assessed with a StatStrip Xpress Glucose/Ketone Meter monitoring system (Nova Biomedical). Mice were considered diabetic after two consecutive measurements >250mg/dl.

In vivo and in vitro T cell assays

For *in vivo* T cell assays, OVA-specific $CD4^+$ T conventional cells from OT-II.*Ly5.1* mice were isolated using $CD4^+$ T cell isolation Kit II (according to the manufacturer's instructions (Miltenyi Biotec)), labeled with Cell Proliferation Dye (CPD) eFluor670 (eBioscience) and i.v. injected (total of $1–2.10^6$ cells/mouse) in WT and *Clec1a* KO mice. One day later, recipient mice were i.p. injected with 100µg of EndoFit OVAprotein (InvivoGen) or with 5.10^7 of UV-C light treated (150mJ/cm²) MCA101-FcROVA cells (expressing membrane-bound OVA and

with no class I MHC expression). After 3 days, spleen was harvested and proliferation (CPD dilution) of injected cells ($CD45.1^+CD4^+$) was assessed by flow cytometry.

For *in vitro* T cells assays, bone marrow cells were cultured (5.10^5 cells/ml) in complete RPMI medium in the presence of 20ng/ml of mouse GM-CSF (Miltenyi Biotec) for 8 days. BMDCs were harvested and incubated in a 96-well plate ($1.25.10^4$ cells per well) with 500µg/ml of EndoFit OVAprotein (InvivoGen), 10µg/ml of $OVA_{323–339}$ (ISQAVHAAHAEINEAGR) peptides (GenScript) or $1,25.10^4$ of UV-C light treated (150mJ/cm²) MCA101-FcROVA cells for 5h. Then, BMDCs were washed 3 times and added ($1,25.10^4$ cells/well) to CPD-labeled purified $CD4^+$ T cells from OT-II.*Ly5.1* mice (5.10^4 cells per well) and proliferation (CPD dilution) was assessed by flow cytometry 3 days later.

FACS data were acquired on a BD FACSCanto™ (BD Biosciences) and analyzed with FlowJo software (Tree Star).

Flow cytometry analysis

Cells were killed by treatment with UV-C light (CL-1000 UV Crosslinker, Analytik Jena) (150mJ/cm²), X-ray (Faxitron CP 160 (Faxitron X-Ray Corp., Wheeling)) (10 Gy for PBMC, 2 for mouse splenocytes) or chemotherapies (staurosporine (1µM Sigma-Aldrich), cisplatin (20µM Merck)) and were subsequently incubated in culture conditions for 18h at 37°C. Mouse splenocytes and human PBMCs were stained with recombinant mouse or human recombinant proteins (5µg/ml) respectively together with fluorescently labeled monoclonal antibodies (mAbs) (anti-CD19 for B, anti-CD3 for T, anti-CD11b for myeloid, anti-NK1.1 and anti-CD56 for NK cells) **(Table S4)**. For Annexin V/PI staining, mouse splenocytes or human PBMCs were stained with mouse or human Fc CLEC-1-AF488 protein (5µg/ml) respectively and with Annexin V (BD Biosciences) and propidium iodide (Sigma-Aldrich) according to manufacturer's instructions. FACS data were acquired on a BD FACSCelesta (BD Biosciences) and analyzed with FlowJo software (Tree Star).

FACS analysis of splenocytes from controls or hepatocarcinoma-burdened livers of WT and *Clec1a* KO mice was conducted using a BD FACSymphony™ flow cytometer and FlowJo v.10 software (Tree Star).

Murine BMDCs generation and stimulation

For *in vitro* BMDCs stimulation, bone marrow cells from WT and *Clec1a* KO mice were cultured (5.10^5 cells/ml) in complete RPMI medium in the presence of 20ng/ml of mouse GM-CSF (Miltenyi Biotec) for 8 days at 37°C and 5% CO_2. Then, BMDCs were stimulated with

UV-C light treated (150mJ/cm²) dead splenocytes at ratio 1:10 respectively ± Poly I:C (20µg/ml) (Invivogen). Cells were harvested, extensively washed and subjected for RNA extraction (at 6h) for Q-PCR analysis **(Table S5)** or for phenotypic analysis (at 24h).

In vitro uptake of dead cells

Splenocytes treated by UV-C light (150 mJ/cm²) were labeled with 25nM of Cell Proliferation Dye (CPD) eFluor670 (Invitrogen) or with 5µM of pH Rodo Red (Molecular Probes) according to the manufacturer's instruction. Bone marrow derived dendritic cells (BMDCs) generated from WT and *Clec1a* KO mice were labeled with 250nM of Cell Proliferation Dye (CPD) eFluor450 (Invitrogen). For uptake of dead cells, BMDCs and dead splenocytes were co-incubated in 96-well culture plate at ratio 1:1 ($2.5.10^5$ cells per well) at various time points (30 to 240 min) at 37°C and 5% CO2. BMDCs were stained with anti-CD11c (PE) and CD11b (PE-Cy7) mAbs and engulfment of dead cells was assessed by flow cytometry.

Gene ontology and pathway enrichment analysis

Pathway enrichment analysis was performed using the Enrichr *(51)* tool based on MSigDB Hallmark 2020 database, using differential expression genes (DEG). Enrichment analyses for gene ontology (GO) were performed with WebGestalt *(52)* tool using. The GO enrichment was performed for biological processes and Benjamini–Hochberg false-discovery rate (FDR) was adopted for screening statistically significance and was set at $FDR < 0.05$. For nSolver™-generated raw counts, DESeq2 R package was used for differential expression analysis between samples *(53)*.

Selection of anti-human CLEC-1 antagonist mAbs

Specificity of anti-hCLEC-1 mAbs (dose-response) was evaluated according to their binding by ELISA on coated recombinant human Fc CLEC-1 protein (Biotechne, 10nM) revealed by anti-mouse IgG-HRP) (0.5µg/ml) and according to their binding by flow cytometry to CLEC-1 expressing cell lines revealed by anti-mouse IgG-PE (5µg/ml).

Antagonist activity of anti-human CLEC1 mAbs was evaluated by flow cytometry by their ability (dose-response) to block the interaction of human Fc CLEC-1-AF488 protein (10µg/ml) to UV-C light treated (150mJ/cm²) necrotic Raji cells.

Fig.S1.

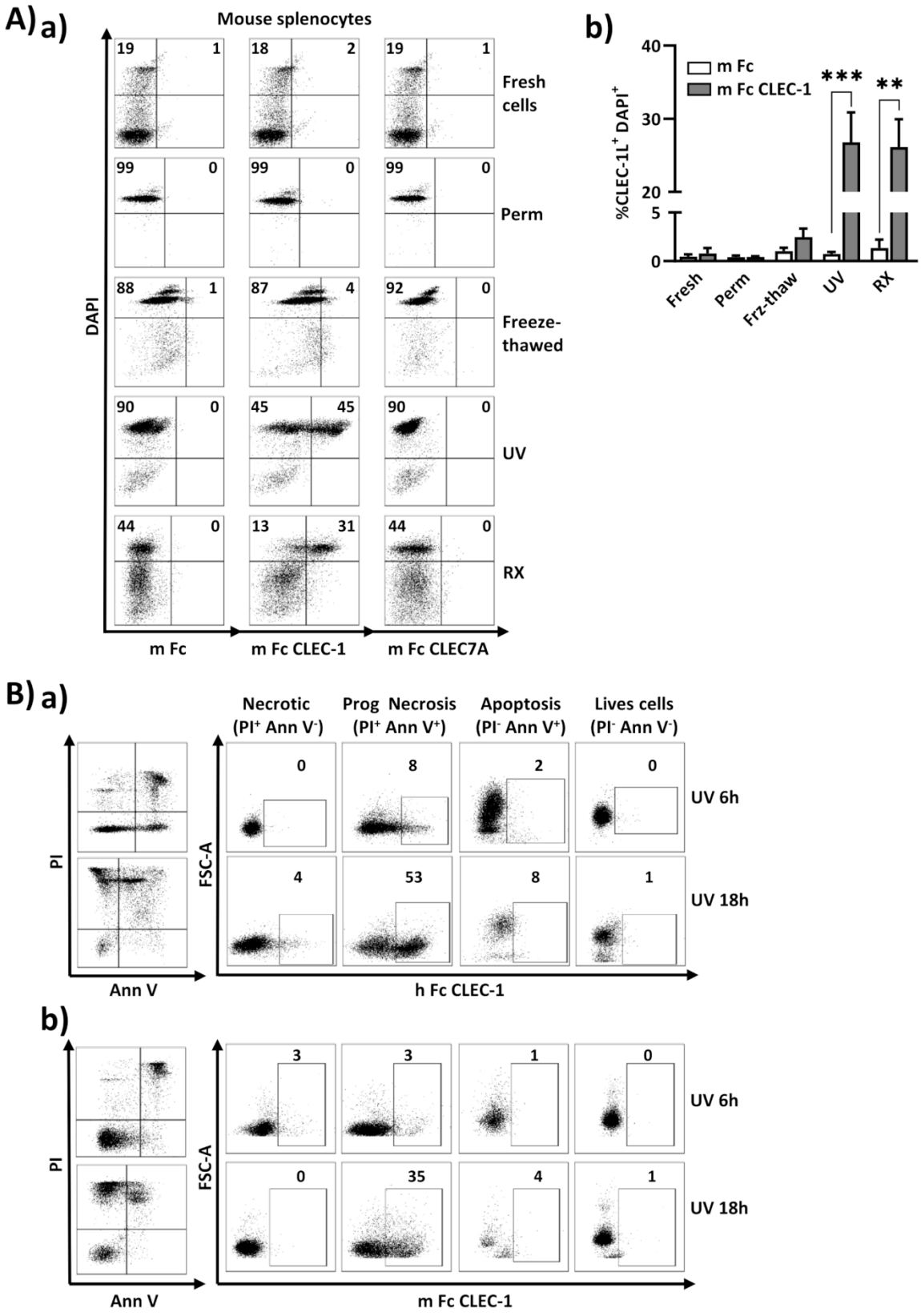

Fig.S1: **Mouse CLEC-1 recognizes intracellular ligands exposed upon programmed necrosis.**

(A) Flow cytometry analysis of mouse splenocytes either fresh, permeabilized, freeze thawing or previously (18h earlier followed by incubation in culture conditions) treated by UV or X-ray (RX), and stained with DAPI and indicated Fc-AF488 fusion proteins or Fc-AF488 alone as control. **(a)** Representative dot plots and **(b)** histograms indicate % of CLEC-1 ligands positive cells in $DAPI^+$ cells (N=5-8, Mean ± SEM, paired t-test **p<0.01, ***p<0.01). **(B)** Flow cytometry analysis of UV-treated **(a)** human PBMCs and **(b)** mouse splenocytes incubated in culture conditions for 6h or 18h, and stained with Annexin V, propidium iodide (PI) and human or mouse Fc CLEC-1 fusion protein respectively.

Fig.S2.

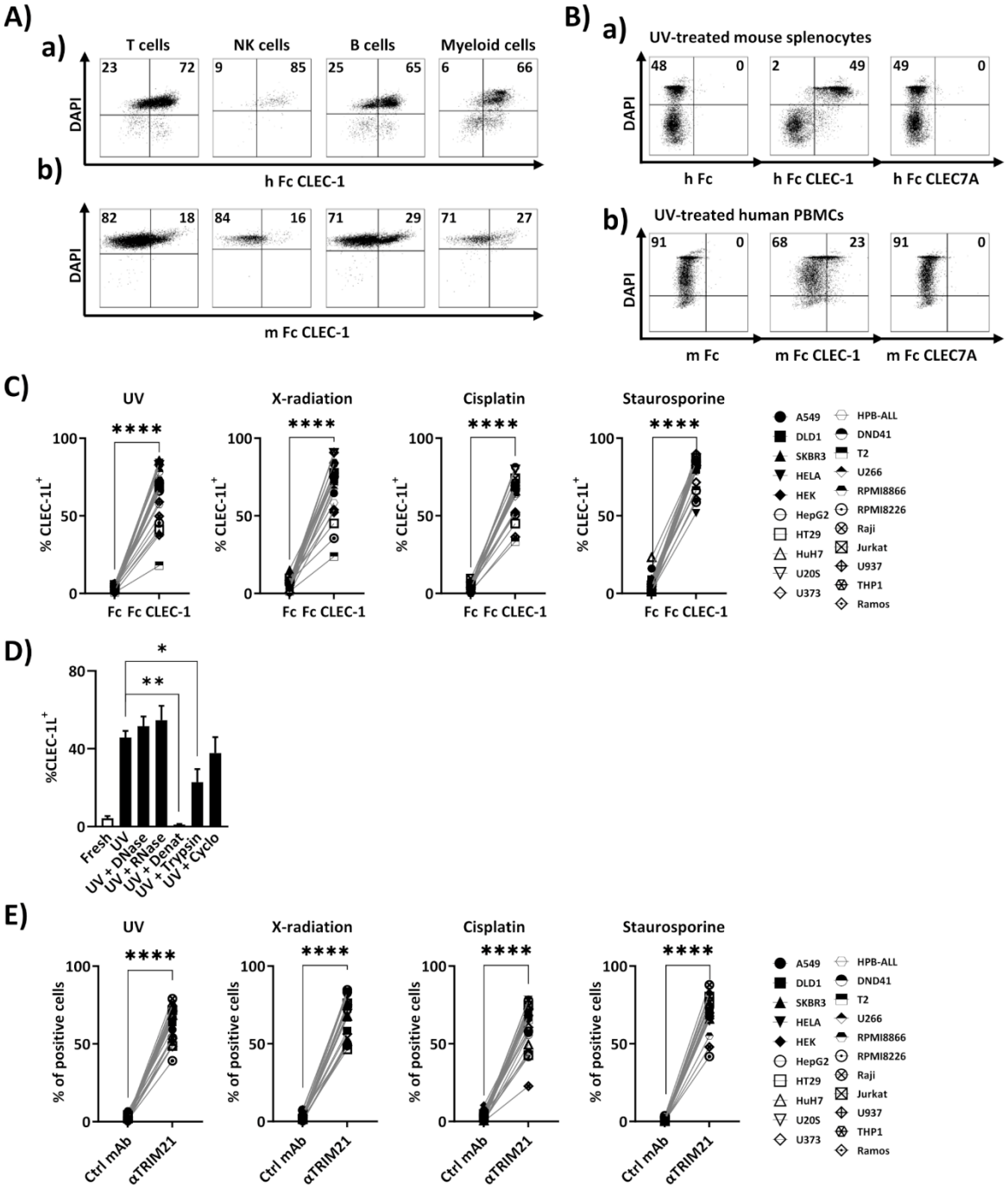

Fig.S2: **CLEC-1 ligands are expressed in all cell types upon programmed necrosis and are conserved between species.**

(A) (a) Human PBMCs and **(b)** mouse splenocytes and previously UV-treated (18h earlier followed by incubation in culture conditions) were stained with cell-type specific mAbs to differentiate T (CD3ε), NK (NK1.1/CD56), B (CD19) and myeloid cells (CD11b). **(B) (a)** mouse splenocytes and **(b)** human PBMCs previously UV-treated (18h earlier followed by incubation in culture conditions) were stained with indicated Fc fusion proteins. Dot plots are representative of at least 3 independent experiments (m:mice, h:human). **(C)** Flow cytometry analysis of human tumor cell lines previously treated with UV or X-ray radiation or with the cytotoxic chemotherapies cisplatin (20µM) or staurosporin (1µM) for 18h in culture conditions

and stained with DAPI and human Fc-CLEC-1 fusion protein or Fc alone as control. Histograms indicate % of CLEC-1 ligands positive cells in $DAPI^+$ cells (n=21, Mean ± SEM, paired t-test ****p<0.001). **(D)** Flow cytometry analysis of fresh or previously UV-treated mouse splenocytes incubated with RNase A (10µg/ml), DNase I (50U/ml), heat-denaturated (20min-65°C) or treated with trypsin (100µg/ml) (30min-37°C) or cycloheximide (100µg/ml) and stained with viability dye and mouse Fc-CLEC-1 fusion protein or Fc alone as control. Histograms indicate MFI staining of CLEC-1 ligand positive cells in dead cells (with MFI of Fc alone subtracted) (N=5-11, Mean ± SEM, paired t-test *p<0.05, **p<0.01). **(E)** Flow cytometry analysis of human tumor cell lines previously treated with UV or X-ray radiation or with the cytotoxic chemotherapies cisplatin (20µM) or staurosporin (1µM) for 18h in culture conditions and stained with anti-human TRIM21 Abs or isotype as control. Histograms indicate % of positive cells (n=21, Mean ± SEM, paired t-test ****p<0.001).

Fig.S3.

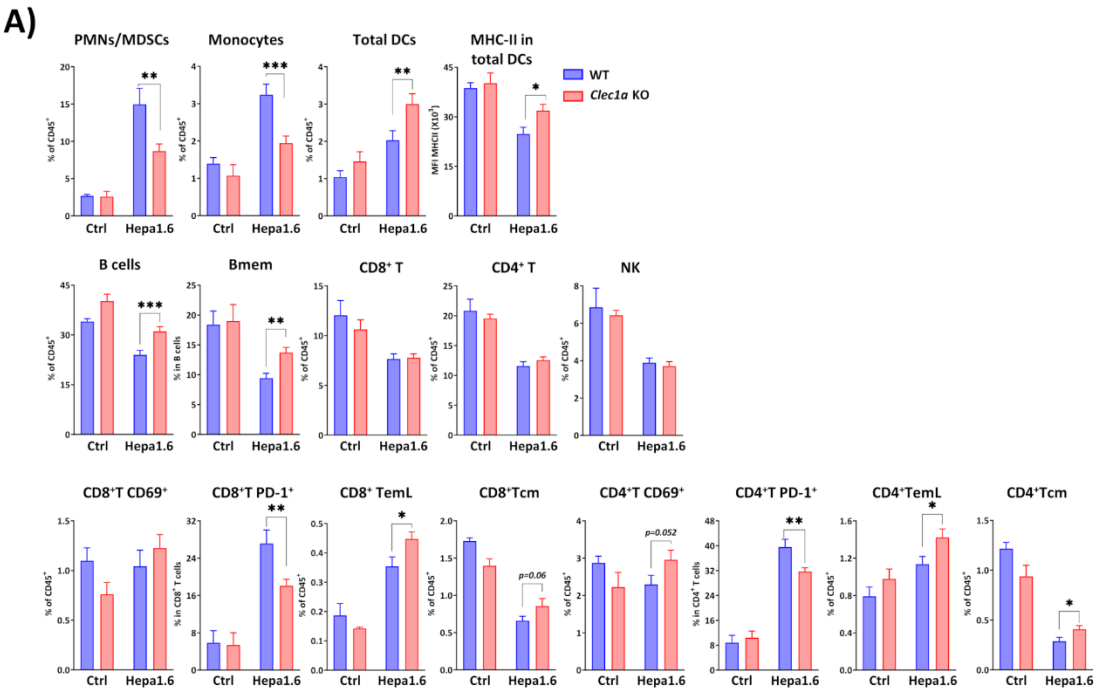

Fig.S3: **Absence of *Clec1a* increases anti-tumor response in spleen in mouse model of Hepa1.6 hepatocarcinoma.**

(A) Flow cytometry analysis of different immune cell subsets representing PMNs/MDSCs ($CD11b^+$ $Ly6G^+$ $MHC\text{-}II^-$), monocytes ($CD11b^+$ $Ly6C^+$ $MHC\text{-}II^-$), total DCs ($CD11c^+$ $MHC\text{-}II^+$), Bmem ($CD19^+$ $CD45R^+$ $CD24^+$ $CD38^-$), TemL ($CD44^+$ $CD62L^-$ $CD27^-$) and Tcm ($CD44^+$ $CD62L^+$) $CD3^+$ $CD4/8^+$ T cells from the spleen of controls (Ctrl) or WT and *Clec1a* KO mice at day 13 after Hepa1.6 inoculation (Data are expressed in % of $CD45^+$ or in particular cell subset) (N=5 for controls, N=15 for Hepa1.6 treated, Mean ± SEM of 3 independent experiments, unpaired t-test *p<0.05, **p<0.01, ***p<0.01).

Fig.S4.

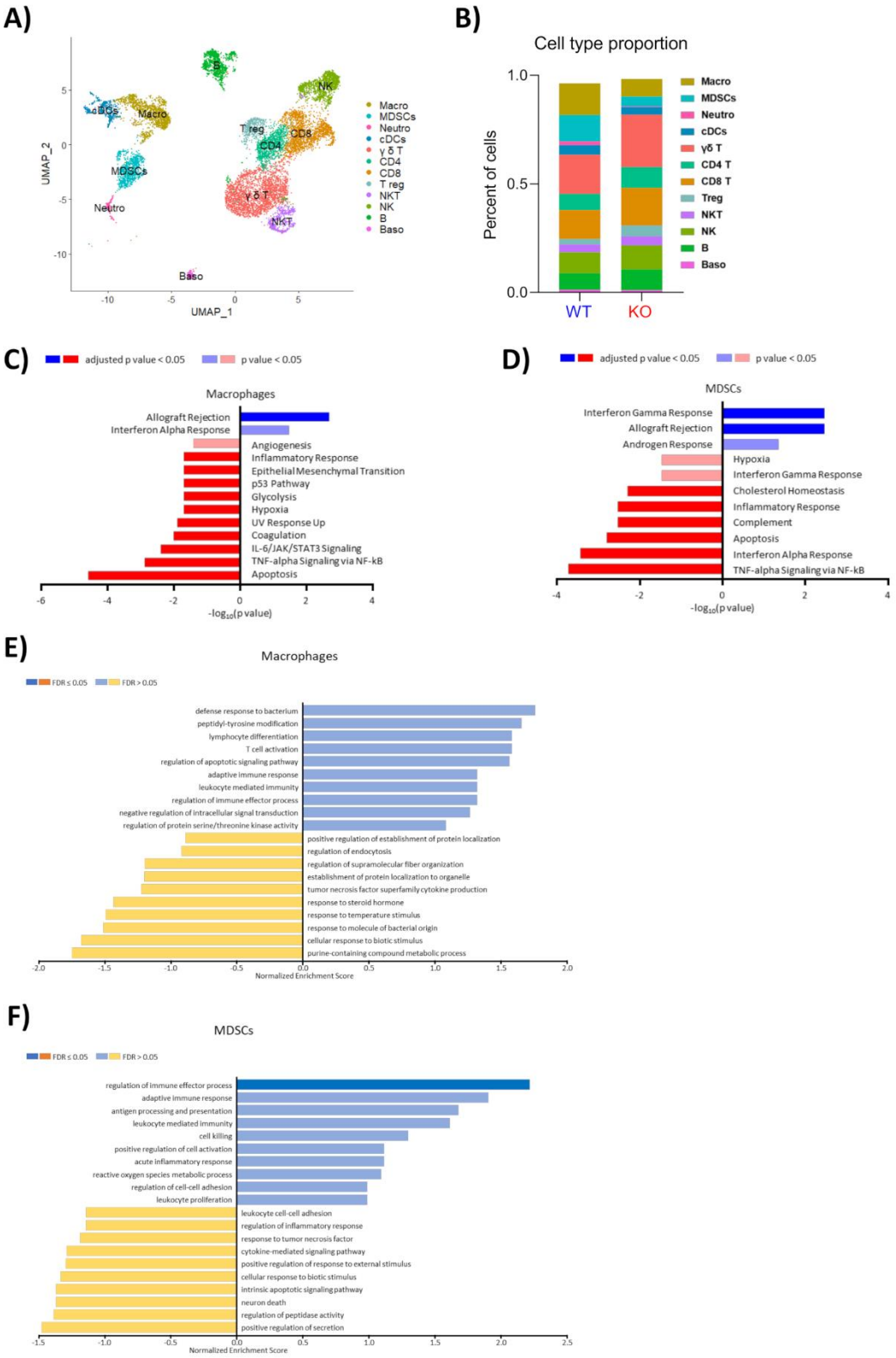

Fig.S4: Single-Cell RNA Sequencing reveals that absence of *Clec1a* modifies the transcriptomic profile of the myeloid TME.

(A) Uniform Manifold Approximation and Projection (UMAP) clustering of the integrated datasets representing the identified cellular clusters (12) (colored by cell type) from tumor-

burdened livers of WT and *Clec1a* KO mice at day 13 post Hepa1.6 tumor inoculation. **(B)** Cell proportion of different cell type distribution by genotype. **(C-D)** Bar chart of overall results of pathways enrichment analysis using Enrichr tool from macrophage and MDSCs from tumor-burdened livers of WT and *Clec1a* KO mice. The blue bars indicate up-regulated pathways, and the red bar indicate down-regulated pathways in *Clec1a* KO mice compared to WT ones. **(E-F)** Bar chart of the GO enrichment analyzed by WebGestalt of macrophages and MDSCs clusters from tumor-burdened livers of WT versus *Clec1a* KO mice.

Fig.S5.

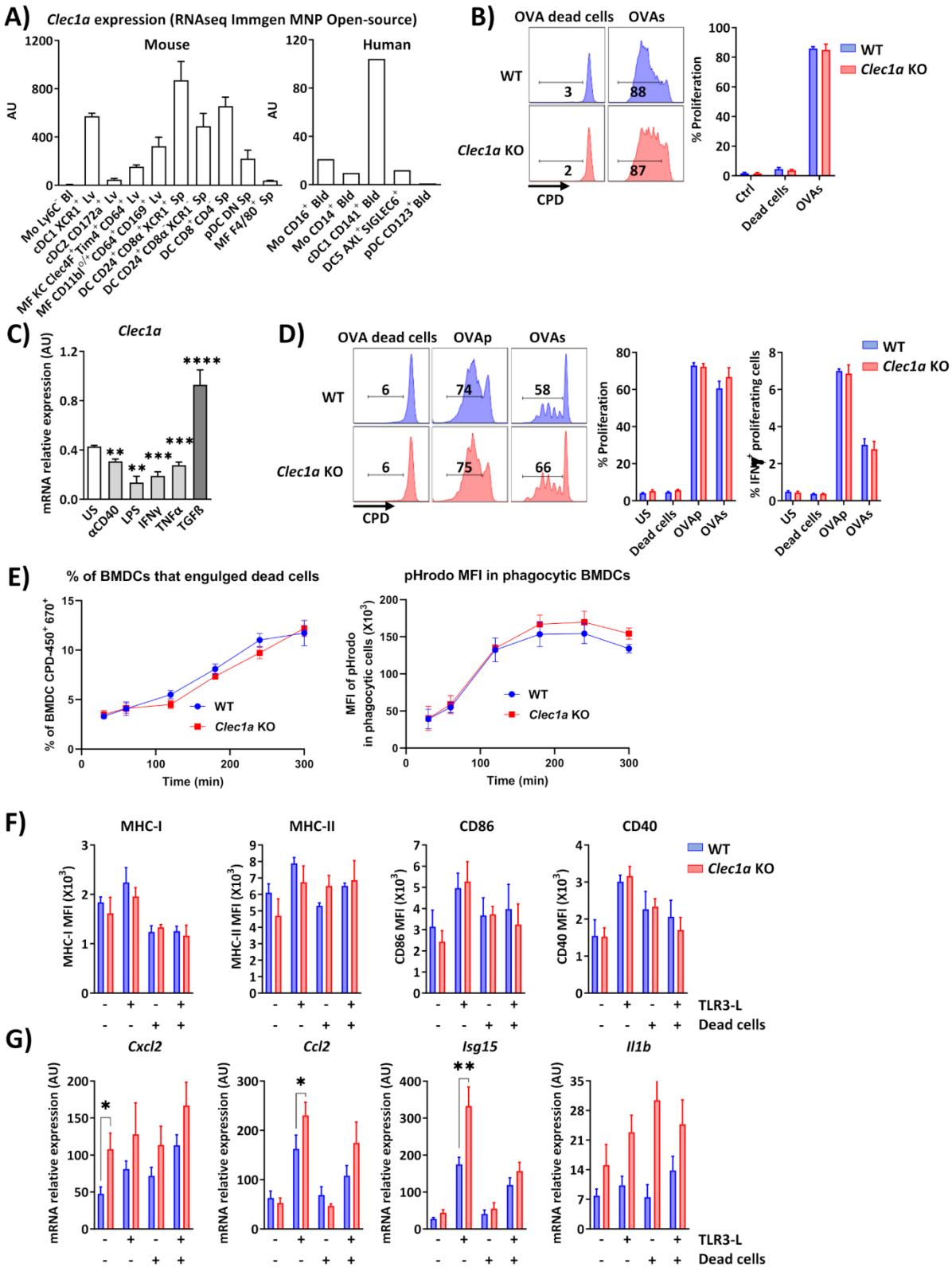

Fig.S5: Loss of CLEC-1 does not influence antigen presentation to CD4+ T cells by DCs nor their maturation but enhances their cytokine and chemokine expression.

(A) *Clec1a* and *CLEC1A* mRNA expression in mouse and human myeloid cell subtypes from ImmGen public RNAseq database (http://www.immgen.org/) (OpenSource Mononuclear

Phagocytes Project for mice, GSE122108) (Bld: Blood, Lv:Liver, Sp: spleen, Mo: monocytes, MF: macrophages, p:plasmacytoid). **(B)** Representative profile and histograms evaluated by flow cytometry of the proliferation (CPD dilution) of splenic OVA-specific $CD4^+$ T (OT-II) cells following *in vivo* inoculation of WT and *Clec1a* KO mice with UV-treated necrotic MCA cells expressing membrane-bound form of OVA (FcROVA) (OVA dead cells) or with soluble OVA protein (OVAs). Control (Ctrl) represents naive mice without OVA injection (N=5-7, Mean ± SEM of two independent experiments). **(C)** *Clec1a* mRNA expression assessed by Q-PCR in mouse BMDCs stimulated (6h) with coated anti-CD40 (10µg/ml), LPS (0.1mg/ml), IFNγ (1µg/ml), TNFα (1000U/ml) and TGFβ (20ng/ml) (data are expressed in arbitrary unit (AU) relative to *Hprt* expression) (N=5-13, Mean ± SEM of 3 independent experiments, paired t-test, **p<0.01, ***p<0.001, ****p<0.0001). **(D)** Representative flow cytometry profile and histograms of the proliferation (reflected by CPD dilution) of OVA-specific $CD4^+$ T (OT-II) cells in response to WT and *Clec1a* KO BMDCs either unstimulated (US) or loaded with UV-treated MCA cells expressing membrane-bound OVA (OVA dead cells), OVA peptide SIINFEKL (OVAp) or soluble OVA (OVAs) (N=5-7, Mean ± SEM of 3 independent experiments). **(E)** CPD eFluor450-labeled BMDCs and CPD eFluor670/pH rodo labeled-dead cells were co-incubated (ratio 1:1) for 30-300 min in culture conditions. Percentage of BMDCs that engulfed dead cells was calculated by the percentage of double positive $CPDe450^+/CPDe670^+$ BMDCs assessed by flow cytometry. Dead cell uptake was quantified by the MFI of pHrodo-labeled dead cells in phagocytic double positive $CPDe450^+/CPDe670^+$ BMDCs assessed by flow cytometry (N=5, Mean ± SEM of 3 independent experiments. **(F)** Flow cytometry analysis of BMDC phenotype (MHC-I, MHC-II, CD86, CD40) from WT and *Clec1a* KO mice stimulated with UV-treated necrotic splenic cells and/or TLR3-L for 24h. Data are expressed in histograms (N=5, Mean ± SEM of 3 independent experiments). **(G)** *Cxcl2*, *Ccl2*, *Isg15*, and *Il1b* mRNA expressions assessed by Q-PCR in BMDCs from WT and *Clec1a* KO mice stimulated with UV-treated necrotic splenic cells and/or TLR3-L for 6h. Results are expressed in histograms (N=9-21, Mean ± SEM of 6 independent experiments in AU of specific cytokine/*Hprt* ratio, paired t-test *p<0.05, **p<0.01).

Fig.S6.

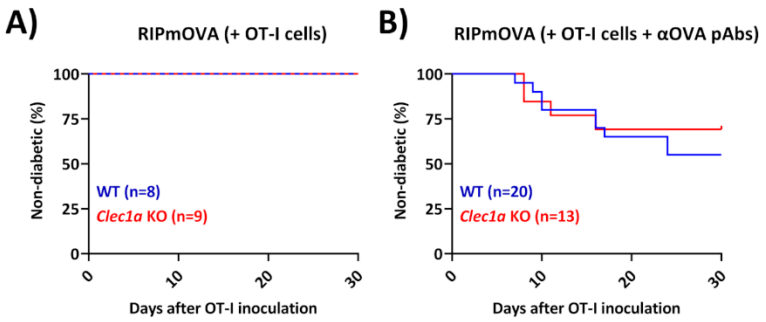

Fig.S6: **Loss of CLEC-1 signaling does not break cross-tolerance following homeostatic cell death.**

Chimeric RIP-mOVA mice reconstituted with bone-marrow from WT or *Clec1a* KO mice were injected with 5.10^6 of OT-I cells alone **(A)** or with rabbit anti-OVA polyclonal IgG (i.p., 0.5mg) **(B)**. Diabetes incidence was assessed by monitoring blood glycemia every other day during at least 12 days (N=8-20, Mean ± SEM).

Fig.S7.

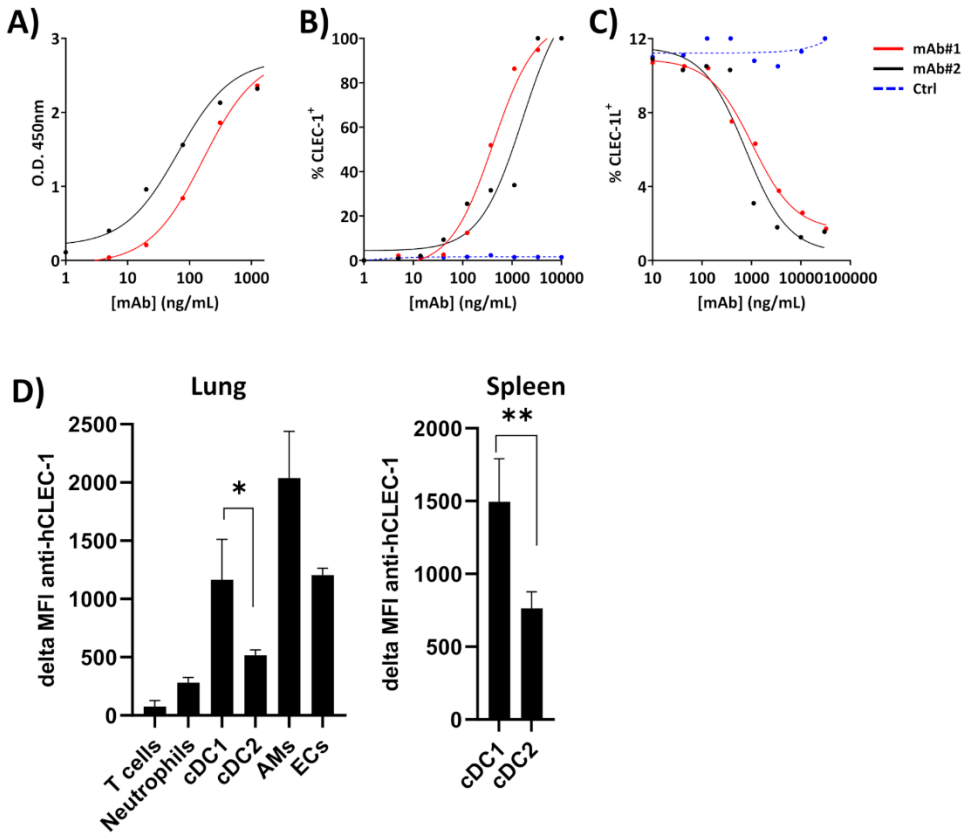

Fig.S7: **Specificity of anti-human CLEC-1 mAbs and expression of CLEC-1 in CLEC-1 humanized mice.**

Specificity of the anti-human CLEC-1 mAbs (#1 and #2) evaluated by **(A)** ELISA on human Fc CLEC-1 and His-CLEC-1 recombinant proteins and by **(B)** flow cytometry on CLEC-1 expressing cell line. **(C)** Antagonism property of mAbs was evaluated by flow cytometry by their dose-dependent potential to block the interaction of human recombinant Fc CLEC-1 protein to UV-treated necrotic PBMCs. **(D)** CLEC-1 expression in T cells ($CD45^+$ $CD3^+$), neutrophils ($CD45^+$ $CD11b^+$ $Ly6G^+$), cDC1 ($CD45^+$ $CD11c^+$ $MHC\text{-}II^{high}$ $XCR1^+$), cDC2 ($CD45^+$ $CD11c^+$ $MHC\text{-}II^{high}$ $CD11b^+$), alveolar macrophages (AP) ($CD45^+$ $CD11b^-$ $CD11c^+$ $CD64^+$) and endothelial cells (ECs) ($CD31^+$ $CD45^-$) from lung and spleen of CLEC-1 humanized mice evaluated by flow cytometry with anti-human CLEC-1 mAb#1. Data are expressed in histograms (delta MFI: substraction of the MFI obtained with isotype control to the specific antibody, N=4-9, Mean ± SEM of 4 independent experiments).

Table S1.

Blood

Cell Type	Markers	WT	*Clec1a*-KO
T cells	$CD3^+$	18,90 ± 3,46	28,00 ± 14,50
$CD4^+$ T cells	$CD3^+CD4^+$	8,33 ± 1,40	15,30 ± 6,71
$CD8^+$ T cells	$CD3^+CD8^+$	9,16 ± 1,74	13,36 ± 5,33
Treg	$CD3^+CD4^+FoxP3^+$	0,54 ± 0,07	0,81 ± 0,17
NK Cells	$CD3^-NK1.1^+$	3,69 ± 0,59	2,14 ± 1,22
B Cells	$CD3^-CD19^+$	54,27 ± 0,80	49,73 ± 10,12
Monocytes	$CD11b^+Ly6c^+$	2,74 ± 0,40	2,42 ± 0,50
Neutrophiles	$CD11b^+Ly6g^+Ly6c^{int}$	8,47 ± 4,46	7,00 ± 3,48
cDCs	$CD11c^+MHC\text{-}II^+$	0,27 ± 0,03	0,26 ± 0,25

Spleen

Cell Type	Markers	WT	*Clec1a*-KO
T cells	$CD3^+$	32.67 ± 4.24	29.03 ± 2.70
$CD4^+$ T cells	$CD3^+CD4^+$	20.87 ± 4.73	18.58 ± 3.96
$CD8^+$ T cells	$CD3^+CD8^+$	11.15 ± 1.54	10.78 ± 1.74
Treg	$CD3^+CD4^+FoxP3^+$	2.27 ± 0.76	2.03 ± 0.51
NK Cells	$CD3^-NK1.1^+$	4.43 ± 1	4.42 ± 0.11
B Cells	$CD3^-CD19^+$	45.60 ± 9.59	50.86 ± 6.62
Monocytes	$CD11b^+Ly6c^+$	1.53 ± 0.42	1.46 ± 0.42
Neutrophiles	$CD11b^+Ly6g^+Ly6c^{int}$	2.96 ± 0.26	2.86 ± 2.25
cDCs	$CD11c^+MHC\text{-}II^+$	1.38 ± 0.33	1.53 ± 0.66
cDC1	$CD11c^+MHC\text{-}II^+CD11b^{-/low}XCR1^+$	0.48 ± 0.17	0.65 ± 0.27
cDC2	$CD11c^+MHC\text{-}II^+CD11b^+XCR1^-$	0.83 ± 0.13	0.73 ± 0.19

Lymph nodes

Cell Type	Markers	WT	*Clec1a*-KO
T cells	$CD3^+$	51.34 ± 9.89	53.60 ± 5.86
$CD4^+$ T cells	$CD3^+CD4^+$	25.27 ± 8.88	28.17 ± 4.54
$CD8^+$ T cells	$CD3^+CD8^+$	21.46 ± 5.59	22.56 ± 4.38
Treg	$CD3^+CD4^+FoxP3^+$	3.46 ± 2.02	4.29 ± 1.19
NK Cells	$CD3^-NK1.1^+$	0.79 ± 0.30	0.58 ± 0.13
B Cells	$CD3^-CD19^+$	26.90 ± 10.42	38.07 ± 4.19
Monocytes	$CD11b^+Ly6c^+$	0.13 ± 0.08	0.14 ± 0.08
Neutrophiles	$CD11b^+Ly6g^+Ly6c^{int}$	0.16 ± 0.11	0.06 ± 0.04
cDCs	$CD11c^+MHC\text{-}II^+$	1.30 ± 0.56	1.15 ± 0.20
cDC1	$CD11c^+MHC\text{-}II^+CD11b^{-/low}XCR1^+$	0.54 ± 0.27	0.44 ± 0.08
cDC2	$CD11c^+MHC\text{-}II^+CD11b^+XCR1^-$	0.41 ± 0.36	0.43 ± 0.13

Table S1: Steady state frequency of most common cell populations in *Clec1a* KO mice.

Table S2.

Blood

Cell Type	Markers	WT	*CLEC1A*-KI
T cells	$CD3^+$	16.24 ± 5.31	15.20 ± 6.29
$CD4^+$ T cells	$CD3^+CD4^+$	6.73 ± 1.90	5.65 ± 0.89
$CD8^+$ T cells	$CD3^+CD8^+$	6.47 ± 1.72	5.87 ± 1.35
Treg	$CD3^+CD4^+FoxP3^+$	0.43 ± 0.1	0.35 ± 0.06
NK Cells	$CD3^-NK1.1^+$	1.83 ± 0.72	1.63 ± 0.81
B Cells	$CD3^-CD19^+$	56.29 ± 13.00	54.52 ± 13.31
Monocytes	$CD11b^+Ly6c^+$	5.18 ± 2.02	5.16 ± 2.40
Neutrophiles	$CD11b^+Ly6g^+Ly6c^{int}$	7.95 ± 3.73	9.47 ± 6.40
cDCs	$CD11c^+MHC\text{-}II^+$	0.85 ± 0.18	0.71 ± 0.42

Spleen

Cell Type	Markers	WT	*CLEC1A*-KI
T cells	$CD3^+$	31,50 ± 3,67	33,70 ± 6,64
$CD4^+$ T cells	$CD3^+CD4^+$	16,07 ± 1,70	17,72 ± 3,24
$CD8^+$ T cells	$CD3^+CD8^+$	12,10 ± 1,71	12,37 ± 2,23
Treg	$CD3^+CD4^+FoxP3^+$	2,49 ± 0,34	2,94 ± 0,71
NK Cells	$CD3^-NK1.1^+$	3,61 ± 0,43	2,26 ± 0,80
B Cells	$CD3^-CD19^+$	52,40 ± 3,16	53,35 ± 5,95
Monocytes	$CD11b^+Ly6c^+$	1,38 ± 0,12	1,21 ± 0,22
Neutrophiles	$CD11b^+Ly6g^+Ly6c^{int}$	1,66 ± 0,71	1,22 ± 0,40
cDCs	$CD11c^+MHC\text{-}II^+$	1,33 ± 0,34	0,88 ± 0,26
cDC1	$CD11c^+MHC\text{-}II^+CD11b^{-/low}XCR1^+$	0,30 ± 0,08	0,19 ± 0,04
cDC2	$CD11c^+MHC\text{-}II^+CD11b^+XCR1^-$	0,91 ± 0,21	0,60 ± 0,19

Lymph nodes

Cell Type	Markers	WT	*CLEC1A*-KI
T cells	$CD3^+$	69,65 ± 4,46	61,03 ± 4,51
$CD4^+$ T cells	$CD3^+CD4^+$	35,70 ± 4,10	31,78 ± 1,96
$CD8^+$ T cells	$CD3^+CD8^+$	30,20 ± 0,57	26,28 ± 3,22
Treg	$CD3^+CD4^+FoxP3^+$	5,74 ± 0,34	5,90 ± 0,40
NK Cells	$CD3^-NK1.1^+$	0,82 ± 0,04	0,50 ± 0,15
B Cells	$CD3^-CD19^+$	25,00 ± 4,67	34,00 ± 4,17
Monocytes	$CD11b^+Ly6c^+$	0,11 ± 0,04	0,08 ± 0,04
Neutrophiles	$CD11b^+Ly6g^+Ly6c^{int}$	0,03 ± 0,02	0,02 ± 0,01
cDCs	$CD11c^+MHC\text{-}II^+$	0,92 ± 0,14	0,55 ± 0,35
cDC1	$CD11c^+MHC\text{-}II^+CD11b^{-/low}XCR1^+$	0,44 ± 0,12	0,25 ± 0,19
cDC2	$CD11c^+MHC\text{-}II^+CD11b^+XCR1^-$	0.41 ± 0.36	0.43 ± 0.13

Table S2: Steady state frequency of most common cell populations in CLEC-1 humanized mice.

Table S3.

Primers	Length (pb)	Sequences 5´-3´	Genotype	Tm (C°)
Clec1a Fw	20	TGCCTTAGTGTGTTGCCTTG	Clec1a WT/KO	62
Clec1a R	20	CGATGTGGATGTGTTTCAGG		
Cre Fw	22	ACCAGGTTCGTTCACTCATGGA	Clec1a WT/KO	62
Cre R	23	GGAACCGAGATGATGTAGCCAGC		
Clec1a Fw	18	AGTCAGAGGCTTCCCTTG	Clec1a WT/KI	58
Clec1a R	18	CGATTTTCTCCAGAGCTC		
CLEC1A_F	19	ATGAACAAAGGTGGCTAT	Clec1a WT/KI	58
CLEC1A_R	18	CGATTTTCTCCAGAGCTC		

Table S3: Primers used for PCR genotyping.

Table S4.

Antibody list

Antibody	Colour	Ref.	Furnisher	Clone	Reactivity
BDCA3	PE	559781	BD	1A4	Hs
CD11b	PB	558123	BD	ICRF44	Hs
CD11c	PE-Cy7	337216	Biolegend	Bu15	Hs
CD19	BV786	563325	BD	SJ25C1	Hs
CD1c	PerCp-eFluor710	46-0015-42	eBioscience	L161	Hs
CD3	BV605	317322	Biolegend	OKT3	Hs
CD56	PE	555516	BD	B159	Hs
HLA-DR	APC-Cy7	335831	BD	L243	Hs
LIN-1	FITC	340546	BD		Hs
CD11b	BUV395	563553	BD	M1/70	Mm
CD11b	PE-Cy7	552850	BD	M1/70	Mm
CD11c	BV711	563048	BD	HL3	Mm
CD19	PE	553786	BD	1D3	Mm
CD19	BV711	563157	BD	1D3	Mm
CD24	APC	562349	BD	M1/69	Mm
CD27	PE	558754	BD	LG.3A10	Mm
CD27	BV605	558754	BD	LG.3A10	Mm
CD279 (PD-1)	BV711	744547	BD	J43	Mm
CD38	PE	553764	BD	90	Mm
CD3ε	PerCP-Cy5.5	551163	BD	145-2C11	Mm
CD4	PE-Cy7	552775	BD	RM4-5	Mm
CD44	BV711	563971	BD	IM7	Mm
CD45	PerCP-Cy5.5	550994	BD	30-F11	Mm
CD45.1	FITC	553775	BD	A20	Mm
CD45.2	BUV395	564616	BD	104	Mm
CD45.2	APC-Cy7	560694	BD	104	Mm
CD45.2	PE	560695	BD	104	Mm
CD45R (B220)	APC-Cy7	561102	BD	RA3-6B2	Mm
CD62L	APC	553152	BD	MEL-14	Mm
CD69	FITC	553236	BD	H1.2F3	Mm
CD8a	BUV737	564297	BD	53-6.7	Mm
CD8a	V450	560469	BD	53-6.7	Mm
CD8a	PE-Cy7	552877	BD	53-6.7	Mm
IFN-γ	PE	554412	BD	XMG1.2	Mm
F4/80	PE	565410	BD	T45-2342	Mm
Fc Block	Purified	553141	BD	2.4G2	Mm
Ly6C	V450	560594	BD	AL-21	Mm
Ly6G	BV605	563005	BD	1A8	Mm
Ly6G	FITC	551460	BD	1A8	Mm
Ly6G	BV605	563005	BD	1A8	Mm
MHCII (I-A/I-E)	FITC	11-5321-82	eBioscience	M5/114.15.2	Mm
MHCII (I-A/I-E)	BV421	562928	BD	AF6-120.1	Mm
MHCI (H2Kb)	FITC	553569	BD	AF6-88.5	Mm
CD80	Percp Cy5.5	560526	BD	16-10A1	Mm
CD86	PE	553692	BD	GL1	Mm
NK-1.1	PercP-Cy5.5	551114	BD	PK136	Mm
NK-1.1	BUV395	564144	BD	PK136	Mm
XCR1	APC	148205	Biolegend	ZET	Mm
XCR1	APC-Cy7	148223	Biolegend	ZET	Mm
VD eFluor506	AmCyan	65-0866	eBioscience		Mm

Table S4: Panels of mAbs used for FACS analysis.

Table S5.

Primers	Length (pb)	Sequences 5´-3´	RNA Source	Tm-3 (C°)
Hprt_Fw	20	AAATGTCAGTTGCTGCGTCC	Mm	73
Hprt_R	20	GCGACAATCTACCAGAGGGT		
Cxcl2_Fw	20	ACTCTCAAGGGCGGTCAAAA	Mm	77
Cxcl2_R	20	CATCAGGTACGATCCAGGCT		
Ccl2_Fw	20	AGGTGTCCCAAAGAAGCTGT	Mm	81
Ccl2_R	20	ACAGAAGTGCTTGAGGTGGT		
Il1b_Fw	20	TCAGGCAGGCAGTATCACTC	Mm	77
Il1b_R	20	AGCTCATATGGGTCCGACAG		
Clec1a_Fw	23	GAGAGCCCTGTCCAATAAGAGTA	Mm	73
Clec1a_R	21	AGGAAGAGCTGGATTTTGCCA		
Isg15_Fw	20	TGGTACAGAACTGCAGCGAG	Mm	79
Isg15_R	20	CTCGAAGCTCAGCCAGAACT		

Table S5: Primers used for Q-PCR amplification.

Data S1: List of DEG genes in macrophages, MDSCs and DCs between tumor burdened livers from WT and *Clec1a* KO mice.

REFERENCES AND NOTES

1. J. Couzin-Frankel, Cancer immunotherapy. *Science* **342**, 1432–1433 (2013).

2. Y. De Vlaeminck, A. González-Rascón, C. Goyvaerts, K. Breckpot, Cancer-associated myeloid regulatory cells. *Front. Immunol.* **7**, 113 (2016).

3. J. P. Böttcher, C. Reis e Sousa, The role of type 1 conventional dendritic cells in cancer immunity. *Trends in Cancer* **4**, 784–792 (2018).

4. T. Shekarian, S. Valsesia-Wittmann, J. Brody, M. C. Michallet, S. Depil, C. Caux, A. Marabelle, Pattern recognition receptors: Immune targets to enhance cancer immunotherapy. *Ann. Oncol.* **28**, 1756–1766 (2017).

5. H. Yan, T. Kamiya, P. Suabjakyong, N. M. Tsuji, Targeting C-type lectin receptors for cancer immunity. *Front. Immunol.* **6**, 408 (2015).

6. E. Chiffoleau, C-type lectin-like receptors as emerging orchestrators of sterile inflammation represent potential therapeutic targets. *Front. Immunol.* **9**, 227 (2018).

7. M. Drouin, J. Saenz, E. Chiffoleau, C-type lectin-like receptors: Head or tail in cell death immunity. *Front. Immunol.* **11**, 251 (2020).

8. P. Thebault, N. Lhermite, G. Tilly, L. Le Texier, T. Quillard, M. Heslan, I. Anegon, J.-P. Soulillou, S. Brouard, B. Charreau, M.-C. Cuturi, E. Chiffoleau, The C-type lectin-like receptor CLEC-1, expressed by myeloid cells and endothelial cells, is up-regulated by immunoregulatory mediators and moderates T cell activation. *J. Immunol.* **183**, 3099–3108 (2009).

9. M. D. L. Robles, A. Pallier, V. Huchet, L. Le Texier, S. Remy, C. Braudeau, L. Delbos, A. Moreau, C. Louvet, C. Brosseau, P. J. Royer, A. Magnan, F. Halary, R. Josien, M. C. Cuturi, I. Anegon, E. Chiffoleau, Cell-surface C-type lectin-like receptor CLEC-1 dampens dendritic cell activation and downstream Th17 responses. *Blood Adv.* **1**, 557–568 (2017).

10. Y. Sobanov, A. Bernreiter, S. Derdak, D. Mechtcheriakova, B. Schweighofer, M. Düchler, F. Kalthoff, E. Hofer, A novel cluster of lectin-like receptor genes expressed in monocytic, dendritic and

endothelial cells maps close to the NK receptor genes in the human NK gene complex. *Eur. J. Immunol.* **31**, 3493–3503 (2001).

11. M. Colonna, J. Samaridis, L. Angman, Molecular characterization of two novel C-type lectin-like receptors, one of which is selectively expressed in human dendritic cells. *Eur. J. Immunol.* **30**, 697–704 (2000).

12. S. Sattler, D. Reiche, C. Sturtzel, I. Karas, S. Richter, M. L. Kalb, W. Gregor, E. Hofer, The human C-type lectin-like receptor CLEC-1 is upregulated by TGF-β and primarily localized in the endoplasmic membrane compartment. *Scand. J. Immunol.* **75**, 282–92 (2012).

13. R. Yoshimi, Y. Ishigatsubo, K. Ozato, Autoantigen TRIM21/Ro52 as a possible target for treatment of systemic lupus erythematosus. *Int. J. Rheumatol.* **2012**, 718237 (2012).

14. V. Davidov, G. Jensen, S. Mai, S. H. Chen, P. Y. Pan, Analyzing one cell at a TIME: Analysis of myeloid cell contributions in the tumor immune microenvironment. *Front. Immunol.* **11**, 1842 (2020).

15. S. Müller, G. Kohanbash, S. J. Liu, B. Alvarado, D. Carrera, A. Bhaduri, P. B. Watchmaker, G. Yagnik, E. Di Lullo, M. Malatesta, N. M. Amankulor, A. R. Kriegstein, D. A. Lim, M. Aghi, H. Okada, A. Diaz, Single-cell profiling of human gliomas reveals macrophage ontogeny as a basis for regional differences in macrophage activation in the tumor microenvironment. *Genome Biol.* **18**, 234 (2017).

16. G. Ghislat, A. S. Cheema, E. Baudoin, C. Verthuy, P. J. Ballester, K. Crozat, N. Attaf, C. Dong, P. Milpied, B. Malissen, N. Auphan-Anezin, T. P. Vu Manh, M. Dalod, T. Lawrence, NF-κB–dependent IRF1 activation programs cDC1 dendritic cells to drive antitumor immunity. *Sci. Immunol.* **6**, 3570 (2021).

17. F. Veglia, E. Sanseviero, D. I. Gabrilovich, Myeloid-derived suppressor cells in the era of increasing myeloid cell diversity. *Nat. Rev. Immunol.* **21**, 485–498 (2021).

18. T. Liuyu, K. Yu, L. Ye, Z. Zhang, M. Zhang, Y. Ren, Z. Cai, Q. Zhu, D. Lin, B. Zhong, Induction of OTUD4 by viral infection promotes antiviral responses through deubiquitinating and stabilizing MAVS. *Cell Res.* **29**, 67–79 (2019).

19. F. Stricher, C. Macri, M. Ruff, S. Muller, HSPA8/HSC70 chaperone protein: Structure, function, and chemical targeting. *Autophagy* **9**, 1937–1954 (2013).

20. K. Hildner, B. T. Edelson, W. E. Purtha, M. Diamond, H. Matsushita, M. Kohyama, B. Calderon, B. U. Schraml, E. R. Unanue, M. S. Diamond, R. D. Schreiber, T. L. Murphy, K. M. Murphy, Batf3 deficiency reveals a critical role for CD8α+ dendritic cells in cytotoxic T cell immunity. *Science* **322**, 1097–1100 (2008).

21. M. L. Broz, M. Binnewies, B. Boldajipour, A. E. Nelson, J. L. Pollack, D. J. Erle, A. Barczak, M. D. Rosenblum, A. Daud, D. L. Barber, S. Amigorena, L. J. Van'tVeer, A. I. Sperling, D. M. Wolf, M. F. Krummel, Dissecting the tumor myeloid compartment reveals rare activating antigen-presenting cells critical for T cell immunity. *Cancer Cell* **26**, 638–652 (2014).

22. S. O. Harbers, A. Crocker, G. Catalano, V. D'Agati, S. Jung, D. D. Desai, R. Clynes, Antibody-enhanced cross-presentation of self antigen breaks T cell tolerance. *J. Clin. Invest.* **117**, 1361–1369 (2007).

23. R. Zilionis, C. Engblom, C. Pfirschke, V. Savova, D. Zemmour, H. D. Saatcioglu, I. Krishnan, G. Maroni, C. V. Meyerovitz, C. M. Kerwin, S. Choi, W. G. Richards, A. De Rienzo, D. G. Tenen, R. Bueno, E. Levantini, M. J. Pittet, A. M. Klein, Single-cell transcriptomics of human and mouse lung cancers reveals conserved myeloid populations across individuals and species. *Immunity* **50**, 1317–1334.e10 (2019).

24. J. Qian, S. Olbrecht, B. Boeckx, H. Vos, D. Laoui, E. Etlioglu, E. Wauters, V. Pomella, S. Verbandt, P. Busschaert, A. Bassez, A. Franken, M. Vanden Bempt, J. Xiong, B. Weynand, Y. van Herck, A. Antoranz, F. M. Bosisio, B. Thienpont, G. Floris, I. Vergote, A. Smeets, S. Tejpar, D. Lambrechts, A pan-cancer blueprint of the heterogeneous tumor microenvironment revealed by single-cell profiling. *Cell Res.* **30**, 745–762 (2020).

25. Z. Tang, C. Li, B. Kang, G. Gao, C. Li, Z. Zhang, GEPIA: A web server for cancer and normal gene expression profiling and interactive analyses. *Nucleic Acids Res.* **45**, W98–W102 (2017).

26. K. Neumann, M. Castiñ Eiras-Vilariñ, U. Hö Ckendorf, N. Hannesschlä Ger, S. Lemeer, D. Kupka, S. Meyermann, M. Lech, H.-J. Anders, B. Kuster, D. H. Busch, A. Gewies, R. Naumann, O. Groß, J. Ruland, Clec12a is an inhibitory receptor for uric acid crystals that regulates inflammation in response to cell death. *Immunity* **40**, 389–399 (2014).

27. C. Del Fresno, P. Saz-Leal, M. Enamorado, S. K. Wculek, S. Martínez-Cano, N. Blanco-Menéndez, O. Schulz, M. Gallizioli, F. Miró-Mur, E. Cano, A. Planas, D. Sancho, DNGR-1 in dendritic cells limits tissue damage by dampening neutrophil recruitment. *Science* **362**, 351–356 (2018).

28. S. Ahrens, S. Zelenay, D. Sancho, P. Hanč, S. Kjær, C. Feest, G. Fletcher, C. Durkin, A. Postigo, M. Skehel, F. Batista, B. Thompson, M. Way, C. Reis e Sousa, O. Schulz, F-actin is an evolutionarily conserved damage-associated molecular pattern recognized by DNGR-1, a receptor for dead cells. *Immunity* **36**, 635–645 (2012).

29. L. Li, J. Wei, R. K. Mallampalli, Y. Zhao, J. Zhao, TRIM21 mitigates human lung microvascular endothelial cells' inflammatory responses to LPS. *Am. J. Respir. Cell Mol. Biol.* **61**, 776–785 (2019).

30. A. Espinosa, V. Dardalhon, S. Brauner, A. Ambrosi, R. Higgs, F. J. Quintana, M. Sjöstrand, M. L. Eloranta, J. N. Gabhann, O. Winqvist, B. Sundelin, C. A. Jefferies, B. Rozell, V. K. Kuchroo, M. Wahren-Herlenius, Loss of the lupus autoantigen Ro52/Trim21 induces tissue inflammation and systemic autoimmunity by disregulating the IL-23-Th17 pathway. *J. Exp. Med.* **206**, 1661–1671 (2009).

31. M. Simoes Eugénio, F. Faurez, G. H. Kara-Ali, M. Lagarrigue, P. Uhart, M. C. Bonnet, I. Gallais, E. Com, C. Pineau, M. Samson, J. Le Seyec, M. T. Dimanche-Boitrel, TRIM21, a new component of the TRAIL-induced endogenous necrosome complex. *Front. Mol. Biosci.* **8**, 139 (2021).

32. R. Yoshimi, T.-H. Chang, H. Wang, T. Atsumi, H. C. Morse, K. Ozato, Gene disruption study reveals a nonredundant role for TRIM21/Ro52 in NF-κB-dependent cytokine expression in fibroblasts. *J. Immunol.* **182**, 7527–7538 (2009).

33. Z. Zhang, M. Bao, N. Lu, L. Weng, B. Yuan, Y. J. Liu, The E3 ubiquitin ligase TRIM21 negatively regulates the innate immune response to intracellular double-stranded DNA. *Nat. Immunol.* **14**, 172–178 (2012).

34. F. Wang, Y. Zhang, J. Shen, B. Yang, W. Dai, J. Yan, S. Maimouni, H. Q. Daguplo, S. Coppola, Y. Gao, Y. Wang, Z. Du, K. Peng, H. Liu, Q. Zhang, F. Tang, P. Wang, S. Gao, Y. Wang, W. X. Ding, G. Guo, F. Wang, W. X. Zong, The ubiquitin E3 ligase TRIM21 promotes hepatocarcinogenesis by suppressing the p62-Keap1-Nrf2 antioxidant pathway. *Cell Mol. Gastroenterol. Hepatol.* **11**, 1369–1385 (2021).

35. Z. Zhao, Y. Wang, D. Yun, Q. Huang, D. Meng, Q. Li, P. Zhang, C. Wang, H. Chen, D. Lu, TRIM21 overexpression promotes tumor progression by regulating cell proliferation, cell migration and cell senescence in human glioma. *Am. J. Cancer Res.* **10**, 114–130 (2020).

36. K. M. Tullett, P. S. Tan, H. Y. Park, R. B. Schittenhelm, N. Michael, R. Li, A. N. Policheni, E. Gruber, C. Huang, A. J. Fulcher, J. C. Danne, P. E. Czabotar, L. M. Wakim, J. D. Mintern, G. Ramm, K. J. Radford, I. Caminschi, M. O'Keeffe, J. A. Villadangos, M. D. Wright, M. E. Blewitt, W. R. Heath, K. Shortman, A. W. Purcel, N. A. Nicola, J. G. Zhang, M. H. Lahoud, RNF41 regulates the damage recognition receptor Clec9a and antigen cross-presentation in mouse dendritic cells. *eLife* **9**, e63452 (2020).

37. S. Gao, H. Wake, M. Sakaguchi, D. Wang, Y. Takahashi, K. Teshigawara, H. Zhong, S. Mori, K. Liu, H. Takahashi, M. Nishibori, Histidine-rich glycoprotein inhibits high-mobility group box-1-mediated pathways in vascular endothelial cells through CLEC-1A. *iScience* **23**, 101180 (2020).

38. Y. Takahashi, H. Wake, M. Sakaguchi, Y. Yoshii, K. Teshigawara, D. Wang, M. Nishibori, Histidine-rich glycoprotein stimulates human neutrophil phagocytosis and prolongs survival through CLEC1A. *J. Immunol.* **206**, 737–750 (2021).

39. A. P. Huffman, J. H. Lin, S. I. Kim, K. T. Byrne, R. H. Vonderheide, CCL5 mediates CD40-driven $CD4^+$ T cell tumor infiltration and immunity. *JCI Insight* **5**, e137263 (2020).

40. C. Denkert, S. Loibl, A. Noske, M. Roller, B. M. Müller, M. Komor, J. Budczies, S. Darb-Esfahani, R. Kronenwett, C. Hanusch, C. Von Törne, W. Weichert, K. Engels, C. Solbach, I. Schrader, M. Dietel, G. Von Minckwitz, Tumor-associated lymphocytes as an independent predictor of response to neoadjuvant chemotherapy in breast cancer. *J. Clin. Oncol.* **28**, 105–113 (2010).

41. J. Canton, H. Blees, C. M. Henry, M. D. Buck, O. Schulz, N. C. Rogers, E. Childs, S. Zelenay, H. Rhys, M. Domart, L. Collinson, A. Alloatti, C. J. Ellison, S. Amigorena, V. Papayannopoulos, D. C. Thomas, F. Randow, C. Reis, The receptor DNGR-1 signals for phagosomal rupture to promote cross-presentation of dead-cell-associated antigens. *Nat. Immunol.* **22**, 140–153 (2021).

42. A. A. Barkal, R. E. Brewer, M. Markovic, M. Kowarsky, S. A. Barkal, B. W. Zaro, V. Krishnan, J. Hatakeyama, O. Dorigo, L. J. Barkal, I. L. Weissman, CD24 signalling through macrophage Siglec-10 is a target for cancer immunotherapy. *Nature* **572**, 392–396 (2019).

43. Y. Ding, Z. Guo, Y. Liu, X. Li, Q. Zhang, X. Xu, Y. Gu, Y. Zhang, D. Zhao, X. Cao, The lectin Siglec-G inhibits dendritic cell cross-presentation by impairing MHC class I-peptide complex formation. *Nat. Immunol.* **17**, 1167–1175 (2016).

44. A. Plato, J. A. Willment, G. D. Brown, C-type lectin-like receptors of the dectin-1 cluster: Ligands and signaling pathways. *Int. Rev. Immunol.* **32**, 134–156 (2013).

45. M. Embgenbroich, S. Burgdorf, Current concepts of antigen cross-presentation. *Front. Immunol.* **9**, 1643 (2018).

46. R. Gazit, P. K. Mandal, W. Ebina, A. Ben-Zvi, C. Nombela-Arrieta, L. E. Silberstein, D. J. Rossi, Fgd5 identifies hematopoietic stem cells in the murine bone marrow. *J. Exp. Med.* **211**, 1315–1331 (2014).

47. I. S. Zeelenberg, W. W. C. van Maren, A. Boissonnas, M. A. Van Hout-Kuijer, M. H. M. G. M. Den Brok, J. A. L. Wagenaars, A. van der Schaaf, E. J. R. Jansen, S. Amigorena, C. Théry, C. G. Figdor, G. J. Adema, Antigen localization controls T cell-mediated tumor immunity. *J. Immunol.* **187**, 1281–1288 (2011).

48. D. McIlroy, B. Barteau, J. Cany, P. Richard, C. Gourden, S. Conchon, B. Pitard, DNA/amphiphilic block copolymer nanospheres promote low-dose DNA vaccination. *Mol. Ther.* **17**, 1473–1481 (2009).

49. R. Satija, J. A. Farrell, D. Gennert, A. F. Schier, A. Regev, Spatial reconstruction of single-cell gene expression data. *Nat. Biotechnol.* **33**, 495–502 (2015).

50. C. Kurts, W. R. Heath, F. R. Carbone, J. Allison, J. F. A. F. Miller, H. Kosaka, Constitutive class I-restricted exogenous presentation of self antigens in vivo. *J. Exp. Med.* **184**, 923–930 (1996).

51. Z. Xie, A. Bailey, M. V. Kuleshov, D. J. B. Clarke, J. E. Evangelista, S. L. Jenkins, A. Lachmann, M. L. Wojciechowicz, E. Kropiwnicki, K. M. Jagodnik, M. Jeon, A. Ma'ayan, Gene set knowledge discovery with enrichr. *Curr. Protoc.* **1**, e90 (2021).

52. Y. Liao, J. Wang, E. J. Jaehnig, Z. Shi, B. Zhang, WebGestalt 2019: Gene set analysis toolkit with revamped UIs and APIs. *Nucleic Acids Res.* **47**, W199–W205 (2019).

53. M. I. Love, W. Huber, S. Anders, Moderated estimation of fold change and dispersion for RNA-seq data with DESeq2. *Genome Biol.* **15**, 550 (2014).